

# 広島大学学術情報リポジトリ

## Hiroshima University Institutional Repository

Title	Reversible Supramolecular System of Porphyrin Exchange between Inclusion in Cyclodextrin and Intercalation in DNA by Change in pH
Author(s)	Notsu, Shota; Sugikawa, Kouta; Ikeda, Atsushi
Citation	Chemistry Select , 3 (21) : 5900 - 5904
Issue Date	2018-06-07
DOI	<a href="https://doi.org/10.1002/slct.201801070">10.1002/slct.201801070</a>
Self DOI	
URL	<a href="http://ir.lib.hiroshima-u.ac.jp/00046210">http://ir.lib.hiroshima-u.ac.jp/00046210</a>
Right	<p>Copyright (c) 2018 Wiley - VCH Verlag GmbH &amp; Co. KGaA, Weinheim</p> <p>This is the accepted version of the following article: S. Notsu, K. Sugikawa, A. Ikeda, Reversible Supramolecular System of Porphyrin Exchange between Inclusion in Cyclodextrin and Intercalation in DNA by Change in pH, Chemistry Select, 3, 5900-5904, 2018, which has been published in final form at <a href="http://doi.org/10.1002/slct.201801070">http://doi.org/10.1002/slct.201801070</a>. This article may be used for non-commercial purposes in accordance with Wiley Self-Archiving Policy. This is not the published version. Please cite only the published version. この論文は出版社版ではありません。引用の際には出版社版をご確認ご利用ください。</p>
Relation	



# Reversible Supramolecular System of Porphyrin Exchange between Inclusion in Cyclodextrin and Intercalation in DNA by Change in pH

Shota Notsu, Kouta Sugikawa, and Atsushi Ikeda\*

**Abstract:** Under the coexistence of cyclodextrin and DNA in water, 5,10,15,20-tetra(4-pyridyl)porphyrin interacted with the cavities of two cyclodextrin molecules in a solution at an around neutral pH and intercalated into DNA under acidic conditions. The supramolecular phenomena occurred completely and reversibly owing to the change in pH.

Porphyrins have been widely used in biological applications, such as inhibitors of human telomerases,<sup>[1]</sup> photosensitizers for photodynamic therapy,<sup>[2,3]</sup> DNA photocleaving agents,<sup>[4]</sup> and as a specific probe of DNA structure.<sup>[5]</sup> To fulfil these important functions porphyrins need to bind strongly with their target biomolecules. Furthermore, the ability to control the amount of porphyrins bound to biomolecules by using external stimuli would be beneficial. Several of these applications involve the interaction of porphyrins with DNA. Three major DNA binding modes have been proposed for the interaction of cationic porphyrins to DNA: (i) intercalation; (ii) outside groove binding; and (iii) outside binding with self-stacking in which porphyrins stack along the DNA helix.<sup>[6]</sup> We have previously demonstrated the exchange of porphyrins between cyclodextrins<sup>[7,8]</sup> and liposomes.<sup>[9]</sup> Other guest molecules, such as azobenzene,<sup>[10]</sup> stilbene,<sup>[10]</sup> and fullerenes<sup>[11]</sup> are released from the cavity of cyclodextrin and transfer into liposomal membranes. In this report, we demonstrated that 5,10,15,20-tetra(4-pyridyl)porphyrin (**1**) complexed with trimethyl- $\beta$ -cyclodextrin (TMe- $\beta$ -CDx; Figure 1) was reversibly transferred to DNA by a pH-dependent switch.

The **1**·TMe- $\beta$ -CDx complex was prepared using a mechanochemical high-speed-vibration milling apparatus.<sup>[3,7]</sup> The UV-vis spectrum of the complex showed an absorption maximum ( $\lambda_{\text{max}}$ ) at 414 nm in water, corresponding to the Soret band of the porphyrin, as well as several other bands at 509, 541, 584, and 640 nm, which were attributed to the Q bands of the porphyrin (Figure 2a, red line). We have already reported that the **1**·TMe- $\beta$ -CDx complex had 1:2 stoichiometry and there were two kinds of

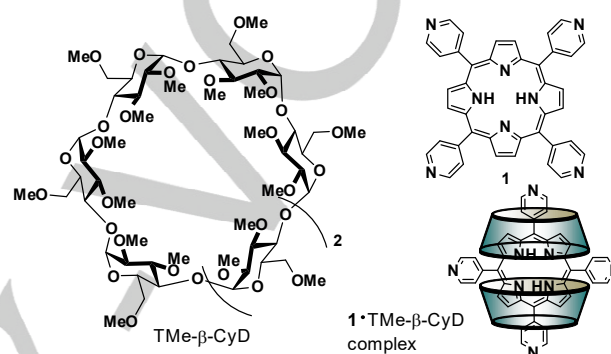
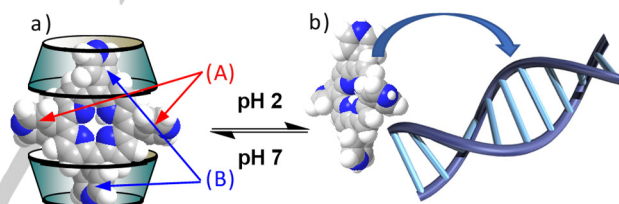


**Figure 1.** Compound structures and schematic illustration of the **1**·TMe- $\beta$ -CDx complex.



**Scheme 1.** Schematic illustration of the porphyrin-exchange reaction between a) cyclodextrins and b) DNA by a change in pH.

pyridyl moieties (Figure 3b):<sup>[3]</sup> two of the pyridyl moieties penetrated the upper rim of each TMe- $\beta$ -CDx (A in Scheme 1a) and the other two were sandwiched by two TMe- $\beta$ -CDxs (B in Scheme 1a). We attempted to determine the association constant ( $K_{\text{ass}}$ ) of the **1**·TMe- $\beta$ -CDx complex at pH 8.3, but failed because the absorption change gave a straight line in the titration (Figure S1). This is because the concentration of **1** was low and free **1** formed self-aggregates owing to its low solubility in water under neutral pH conditions. Therefore, the  $K_{\text{ass}}$  value was determined under acidic conditions (pH 2.1). A plot of the proportion of **1** versus [TMe- $\beta$ -CDx] gave a sigmoidal curve,<sup>[12]</sup> which indicated that the inclusion of **1** in two TMe- $\beta$ -CDxs occurred according to a well-defined cooperative phenomenon (Figure S2a). The TMe- $\beta$ -CDx-binding profile of this complex was analysed using the Hill equation:  $\log[y/(1-y)] = n \log[\text{TMe-}\beta\text{-CDx}] - \log K_{\text{ass}}$ , in which  $K_{\text{ass}}$  and  $n$  are the association constant and Hill coefficients, respectively, and  $y = K_{\text{ass}}/([1] - n - K_{\text{ass}})$ .<sup>[13]</sup>

S. Notsu, Dr. K. Sugikawa, Prof. A. Ikeda  
Department of Applied Chemistry, Graduate School of Engineering  
Hiroshima University  
1-4-1 Kagamiyama, Higashi-Hiroshima 739-8527, Japan  
E-mail: aikeda@hiroshima-u.ac.jp

Supporting information for this article is given via a link at the end of the document.

From the slope and the intercept of the linear plot in the range of  $[TMe-\beta-CDx] = 0.5\text{--}5.2\text{ mM}$ , we obtained a  $K_{ass}$  value of 380 for the **1**•TMe- $\beta$ -CDx complex (correlation coefficient 0.990), together with an  $n$  value of 1.4 (Figure S2b). Although the details for the cooperative phenomenon are not clear at present, it was considered that a steric hindrance of inclusion in one TMe- $\beta$ -CDx inhibited the rotation of the two pyridyl

moieties (A in Scheme 1a) and second inclusion of another TMe- $\beta$ -CDx was accelerated because the loss of the Gibbs energy decreased (Scheme S1).

The absorption maximum shifted to 431 nm after mixing the complex with salmon sperm DNA in aqueous solution at 30 °C (Figure 2a, blue line). Because the shift of the Soret band of 5,10,15,20-tetra(*N*-methylpyridinium-4-yl)porphyrin (TMPyP) has been shown to represent intercalation of TMPyP into DNA (436 nm)<sup>[14]</sup> the observed Soret shift indicated that **1** also intercalated into DNA. The pH of the mixture was 2.7 because the DNA solution used in this paper was acidic and a buffer was not used. We investigated the pH dependence of the UV-vis absorption spectra of the mixture of the **1**•TMe- $\beta$ -CDx complex and DNA (Figure 2b). Based on the pH titration, **1** was gradually protonated and intercalated in DNA at a pH below 5 (Figure 2b inset). To confirm the possibility of protonation of a pyrrole moiety in **1** under acidic conditions, the UV-vis spectrum of the **1**•TMe- $\beta$ -CDx complex was measured at pH 2.3 by the addition of HCl in H<sub>2</sub>O in the absence of DNA. The spectrum of the **1**•TMe- $\beta$ -CDx complex at pH 2.3 showed very minor changes from that at pH 7 (Figure 2c), indicating that the pyrrole moiety in **1** was not protonated. Consequently, the result clearly shows that the  $pK_b$  of the pyrrole moiety in **1** was  $< \text{pH } 2.1$ . This result is consistent with the report that the  $pK_b$  of a pyrrole moiety in 5,10,15,20-tetrakis(*N*-methylpyridinium-4-yl)porphyrin is 1.4.<sup>[15]</sup>

To remove the influence of pH, the UV-vis spectrum was measured in a 0.2 M phosphate buffer solution (pH 6.8) containing the **1**•TMe- $\beta$ -CDx complex and DNA. The result showed that no spectral change was observed (Figure S3). In the <sup>1</sup>H NMR spectrum, the peaks assigned to the **1**•TMe- $\beta$ -CDx complex remained unchanged after mixing with DNA at pH 7.0 (Figure 3c). The result indicated that **1** did not transfer from two TMe- $\beta$ -CDx cavities (Figure 1) to DNA under neutral pH conditions. Therefore, we anticipated that **1** should return to the cavities of the two TMe- $\beta$ -CDxs after changing from acidic conditions to neutral pH conditions. After returning the solution to neutral pH conditions by the addition of NaOH in H<sub>2</sub>O (pH 6.8), the absorption spectrum reverted to a spectrum that was similar to that recorded for the **1**•TMe- $\beta$ -CDx complex (Figure 2a, green line). The spectral changes were repeatedly reversible by the addition of HCl or NaOH in H<sub>2</sub>O (Figure 2a inset). The both exchange rates at pH 2.8 and 6.8 were very fast because the solution color changed immediately between brown and purple by pH changes.

<sup>1</sup>H NMR spectra (Figures 3 and S4-S8) were obtained to confirm if all of the porphyrins were released from the two TMe- $\beta$ -CDx cavities after mixing DNA in D<sub>2</sub>O at 30 °C for 1 h. In the absence of DNA, the peaks corresponding to the **1**•TMe- $\beta$ -CDx complex in the NMR spectrum were observed (red and blue circles in Figure 3b and Figure S5a). In contrast, no peaks could be assigned to the **1**•TMe- $\beta$ -CDx complex following the addition of DNA (Figures 3c and S6). These

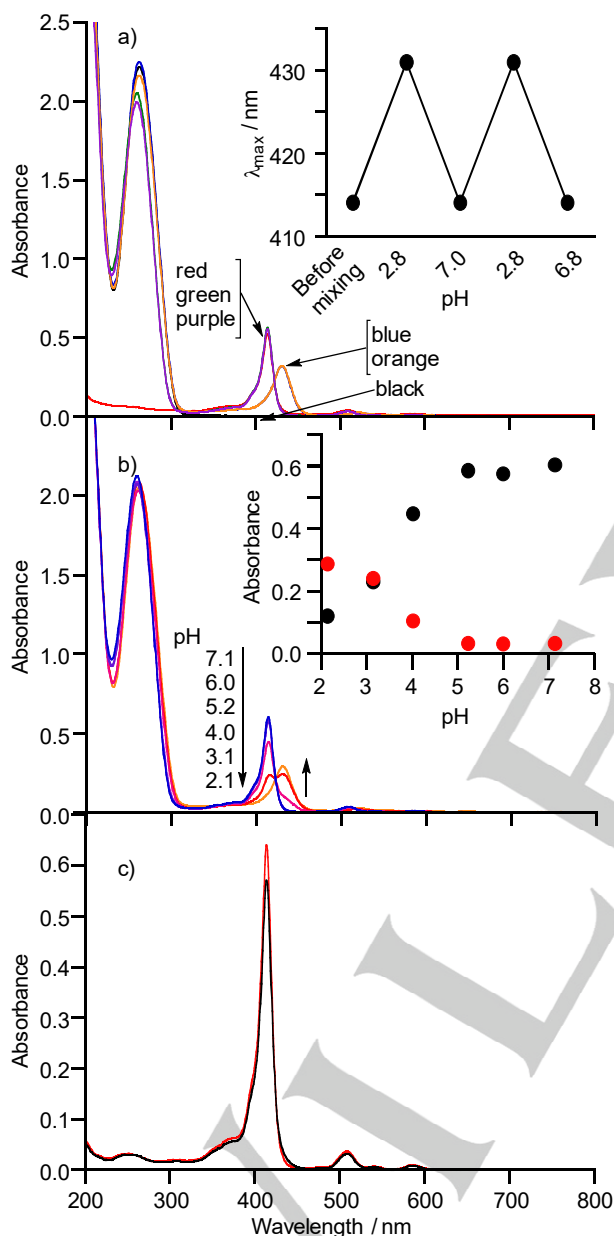


**Figure 2.** UV-vis absorption spectra of a) DNA (black line), the **1**•TMe- $\beta$ -CDx complex before mixing with DNA (red line) and the **1**•TMe- $\beta$ -CDx complex after mixing with DNA (pH 2.8, blue line), after adding NaOH (pH 7.0, green line), after adding HCl (pH 2.8, orange line) and after adding NaOH (pH 6.8, purple line). Inset:  $\lambda_{max}$  of the Soret band versus pH change. b) UV-vis absorption spectra of the mixture of the **1**•TMe- $\beta$ -CDx complex and DNA at pH 7.1, 6.0, 5.2, 4.0, 3.1, and 2.1. Inset: absorbance of the Soret band versus pH at 414 (black circles) and 431 (red circles) nm. c) The **1**•TMe- $\beta$ -CDx complex (pH 6.9, black line) and after adding HCl (pH 2.3, red line).

results clearly indicated that **1** was released completely from the TMe- $\beta$ -CDx cavities. Particular peaks belonging to **1** could have broadened, such as the peak at 8.9 ppm, and/or overlapped with the peaks arising from DNA. Peak broadening suggested that the molecular motions of **1** were suppressed by intercalation into DNA because of the formation of a high molecular weight species or a self-aggregation process. Furthermore, the peaks corresponding to the **1**•TMe- $\beta$ -CDx complex reappeared after returning to neutral pD conditions following the addition of NaOD in D<sub>2</sub>O (pD 6.8)<sup>[16]</sup> (red and blue circles in Figure 3d and Figure S7). The result clearly showed that **1** re-interacts with two TMe- $\beta$ -CDx cavities (Scheme 1). The peaks corresponding to the **1**•TMe- $\beta$ -CDx complex were present in the 0.2 M phosphate buffer solution (pD 6.8) (red and blue circles in Figure 3e and Figure S8), which showed that **1** was scarcely released from the two TMe- $\beta$ -CDx cavities under neutral pD conditions.

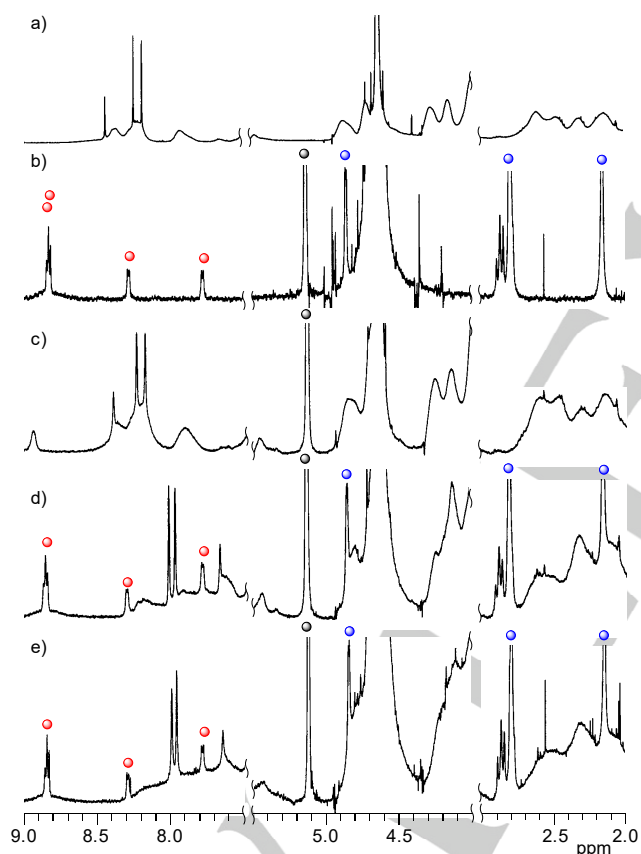


**Figure 3.** Partial <sup>1</sup>H NMR spectra of a) DNA, b–d) the **1**•TMe- $\beta$ -CDx complex b) before and c) and d) after mixing with DNA at 30 °C for 1 h (pD 2.7) and d) after the addition of NaOD in D<sub>2</sub>O (pD 6.8) and e) the **1**•TMe- $\beta$ -CDx complex after mixing with DNA at 30 °C for 1 h in 0.2 M phosphate buffer solution (pD 6.8) ([**1**] = 0.25 mM, [TMe- $\beta$ -CDx] = 4.49 mM and [base pair of DNA] = 32.5 mM). (●: free TMe- $\beta$ -CDx, ●: TMe- $\beta$ -CDx in the **1**•TMe- $\beta$ -CDx complex, and ●: **1** in the **1**•TMe- $\beta$ -CDx complex).

The intercalation of **1** into DNA can be confirmed by inhibiting the intercalation of ethidium bromide (EB) into DNA. EB

has a strong fluorescence intensity upon intercalation into DNA.<sup>[17]</sup> Therefore, the inhibition of the intercalation of EB into DNA by other intercalators should lead to a decrease in the fluorescence intensity arising from the intercalation of EB into DNA.<sup>[15]</sup> As shown in Figure 4a, the fluorescence intensity of EB in the mixture of EB and DNA (black line) decreased upon addition of the **1**•TMe- $\beta$ -CDx complex under acidic conditions (pH 2.8) (red line), suggesting that **1** intercalates partly into DNA (Scheme 1). In contrast, when **1** was scarcely released from the two TMe- $\beta$ -CDx cavities in a 0.2 M phosphate buffer solution (pH 6.8), the fluorescence intensity of EB also barely changed (Figure 4b).

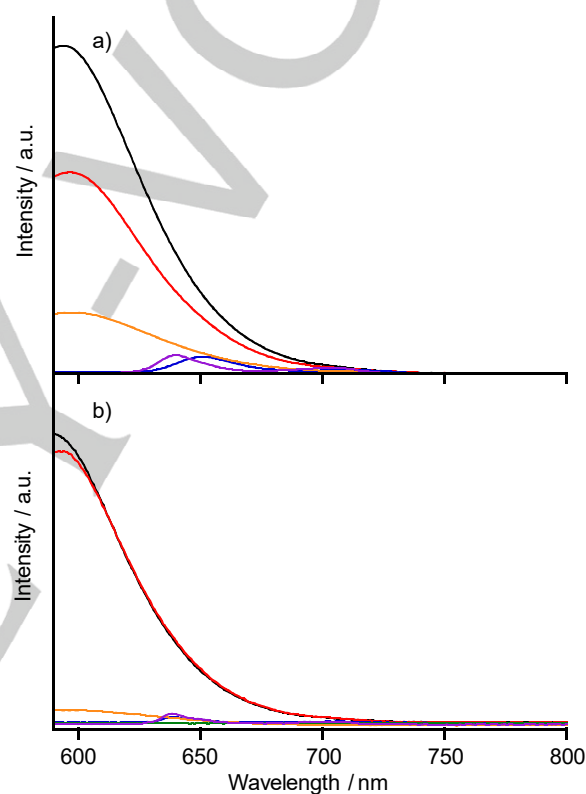


**Figure 4.** Fluorescence spectra of EB with DNA (black line), with a mixture of DNA and **1**•TMe- $\beta$ -CDx complex (red line) and without DNA (orange line), DNA only (green line) and the **1**•TMe- $\beta$ -CDx complex before and after mixing with DNA (purple and blue lines, respectively) under a) acidic conditions (pH 2.8) and b) neutral conditions [a 0.2 M phosphate buffer solution (pH 6.8)].

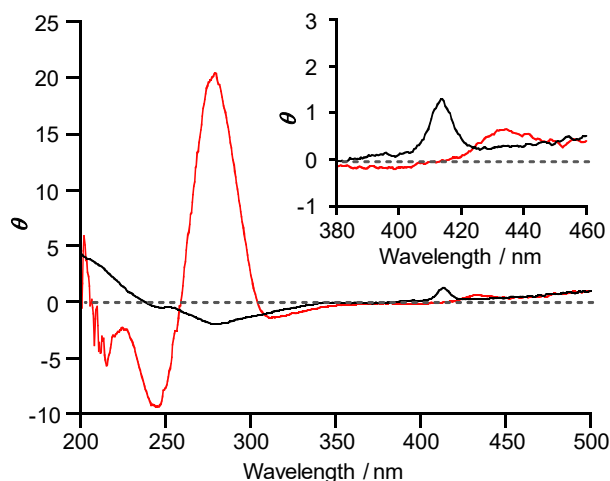


**Figure 5.** CD spectra of the **1**•TMe- $\beta$ -CDx complex before (black line) and after mixing with DNA at 30 °C for 1 h (pH 2.7, red line) (1 mm cell, 25 °C). The inset shows the 380–460 nm region.

Under acidic conditions, there is a possibility that cationic **1** dissolves in water alone after it is released from the cavities of CDxs. Circular dichroism (CD) spectra were recorded in an aqueous solution to confirm the intercalation of **1** into chiral DNA. Before mixing with DNA, **1** gave an induced CD (ICD) at 414 nm owing to the chiral TMe- $\beta$ -CDx (Figure 5 black line). After mixing with DNA, although the  $\lambda_{\max}$  shifted from 414 to 434 nm, the ICD of **1** remained despite the release of the chiral TMe- $\beta$ -CDxs from the cavities (Figure 5 red line). We investigated the pH dependence of the CD spectra of the mixture of the **1**•TMe- $\beta$ -CDx complex and DNA by the addition of NaOH in H<sub>2</sub>O (Figure S9). Based on the pH titration, the ICD at 434 decreased and the ICD at 414 nm increased with a rise in pH (Figure S9 inset). The CD spectrum at pH 7.1 (Figure S9 inset, black line) was similar to that of **1**•TMe- $\beta$ -CDx complex (Figure 5 inset, black line). These ICD spectra were not observed in a DNA solution in the absence of **1** (Figure S10). The result indicated that **1** still existed in the asymmetric field, *i.e.*, **1** intercalated into the chiral DNA (Scheme 1).

In the absence of DNA, the <sup>1</sup>H NMR spectrum of the **1**•TMe- $\beta$ -CDx complex gave sharp peaks, which were assigned to free **1**. We assumed that compound **1** was released from TMe- $\beta$ -CDx at pH 1.0 because the spectrum was the same as that of pure **1** at pH 1.0 (Figure S5c and d). The peak broadening of **1** at pH 2.0 in the presence of DNA indicated that there was an equilibrium between the complex and free **1** (Figure S5b). These results clearly showed that the **1**•TMe- $\beta$ -CDx complex was unstable under acidic conditions because peak broadening was caused by coalescence between the free and complex states at pH 2.0 and dissociated because no peaks could be assigned to TMe- $\beta$ -CDx in the **1**•TMe- $\beta$ -CDx complex, whereas at pH 1.0 the peaks could be assigned to free **1**. The reason for the decomposition of the complex was an increase in the

hydrophobicity and the generation of cations by protonation of the 4-pyridyl moieties of **1**. Cationic porphyrins are known to form unstable complexes with TMe- $\beta$ -CDx,<sup>[8]</sup> but the spontaneous aggregation of **1** under acidic conditions had not been considered. Furthermore, protonated **1** can interact through electrostatic interactions, as observed for the interaction between TMPyP and DNA.<sup>[14]</sup> Here, the protonation of **1** led to the destabilisation of the reactant and the stabilisation of the product. Both factors promoted the reaction.

In summary, compound **1** in the **1**•TMe- $\beta$ -CDx complex was released from two TMe- $\beta$ -CDx cavities and intercalated into DNA under acidic conditions. A cationic **1** born by protonation of the 4-pyridyl moiety causes destabilisation of the **1**•TMe- $\beta$ -CDx complex and stabilisation of the intercalation of **1** into anionic DNA, as observed previously for TMPyP. However, in contrast to this previous study, the DNA-intercalated **1** returned to the TMe- $\beta$ -CDx cavities under neutral pH conditions. The release of **1** from DNA occurred because of the stabilisation of the **1**•TMe- $\beta$ -CDx complex and destabilisation of **1** intercalated into anionic DNA. The reaction was repeatedly reversible by changing the pH.

## Supporting Information Summary

The supporting information includes experimental details regarding to the materials, preparation of the mixture of the **1**•TMe- $\beta$ -CDx complex with DNA, and measurements. The the inhibition of the rotation of the pyridyl moieties in **1** by complexation of TMe- $\beta$ -CDx, Hill plots, complete NMR spectra of Figure 3, UV-vis absorption spectra of the **1**•TMe- $\beta$ -CDx complex in buffer solution, and CD spectra of the mixture of the **1**•TMe- $\beta$ -CDx complex with DNA and DNA alone can also be found in the supporting information.

## Acknowledgements

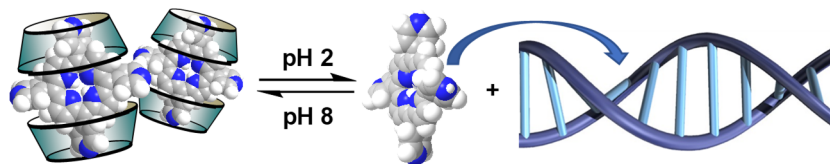
This work was supported by a JSPS KAKENHI Grant-in-Aid for Scientific Research (B) (Grant No. JP16H04133) and a Grant-in-Aid for Challenging Exploratory Research (Grant No. JP16K13982). We thank Zoran Dinev, PhD, from Edanz Group ([www.edanzediting.com/ac](http://www.edanzediting.com/ac)) for editing a draft of this manuscript.

**Keywords:** cyclodextrins • DNA • host-guest systems • intercalator • porphyrins

- [1] a) I. Haq, J. O. Trent, B. Z. Chowdhry, T. C. Jenkins, *J. Am. Chem. Soc.* **1999**, *121*, 1768–1779; b) L. H. Hurley, R. T. Wheelhouse, D. Sun, S. M. Kerwin, M. Salazar, O. Y. Fedoroff, F. X. Han, H. Han, E. Izbiccka, D. D. Von Hoff, *Pharmacol. Ther.* **2000**, *85*, 141–158.  
[2] a) E. D. Sternberg, D. Dolphin, *Tetrahedron* **1998**, *54*, 4151–4202; b) D. K. Chatterjee, L. S. Fong, Y. Zhang, *Adv. Drug Delivery Rev.* **2008**, *60*, 1627–1637; c) S. Yano, S. Hirohara, M. Obata, Y. Hagiya, S.; Ogura, A.

- Ikeda, H. Kataoka, M. Tanaka, T. Joh, *J. Photochem. Photobiol., C* **2011**, *12*, 46–67.
- [3] A. Ikeda, S. Satake, T. Mae, M. Ueda, K. Sugikawa, H. Shigeto, H. Funabashi, A. Kuroda, *ACS Med. Chem. Lett.* **2017**, *8*, 555–559.
- [4] a) W. K. Pogozelski, T. D. Tullius, *Chem. Rev.* **1998**, *98*, 1089–1107; b) C. J. Burrows, J. G. Muller, *Chem. Rev.* **1998**, *98*, 1109–1151; c) B. Armitage, *Chem. Rev.* **1998**, *98*, 1171–1200.
- [5] E. Di Mauro, R. Saladino, P. Tagliatesta, V. De Sanctis, R. Negri, *J. Mol. Biol.* **1998**, *282*, 43–57.
- [6] a) R. F. Pasternack, E. J. Gibbs, *Met. Ions Biol. Syst.* **1996**, *33*, 367–397; b) N. E. Mukundan, G. Petho, D. W. Dixon, L. G. Marzilli, *Inorg. Chem.* **1995**, *34*, 3677–3687; c) J. E. McClure, L. Baudouin, D. Mansuy, L. G. Marzilli, *Biopolymers* **1997**, *42*, 203–217; d) A. B. Guliaev, N. B. Leontis, *Biochemistry* **1999**, *38*, 15425–15437.
- [7] a) Y. Tsuchiya, T. Shiraki, T. Matsumoto, K. Sugikawa, K. Sada, A. Yamano, S. Shinkai, *Chem. Eur. J.* **2012**, *18*, 456–465; b) Y. Tsuchiya, A. Yamano, T. Shiraki, K. Sada, S. Shinkai, *Chem. Lett.* **2011**, *40*, 99–101.
- [8] K. Kano, N. Tanaka, H. Minamizono, Y. Kawakita, *Chem. Lett.* **1996**, *25*, 925–926.
- [9] A. Ikeda, S. Hino, T. Mae, Y. Tsuchiya, K. Sugikawa, M. Tsukamoto, K. Yasuhara, H. Shigeto, H. Funabashi, A. Kuroda, M. Akiyama, *RSC Adv.* **2015**, *5*, 105279–105287.
- [10] A. Ikeda, S. Hino, K. Ashizawa, K. Sugikawa, J. Kikuchi, M. Tsukamoto, K. Yasuhara, *Org. Biomol. Chem.* **2015**, *13*, 6175–6182.
- [11] a) A. Ikeda, T. Sato, K. Kitamura, K. Nishiguchi, Y. Sasaki, J. Kikuchi, T. Ogawa, K. Yogo, T. Takeya, *Org. Biomol. Chem.*, **2005**, *3*, 2907–2909; b) A. Ikeda, Y. Doi, M. Hashizume, J. Kikuchi, T. Konishi, *J. Am. Chem. Soc.*, **2007**, *129*, 4140–4141; c) A. Ikeda, M. Mori, K. Kiguchi, K. Yasuhara, J. Kikuchi, K. Nobusawa, M. Akiyama, M. Hashizume, T. Ogawa, T. Takeya, *Chem. Asian J.* **2012**, *7*, 605–613; d) A. Ikeda, T. Mae, M. Ueda, K. Sugikawa, H. Shigeto, H. Funabashi, A. Kuroda, M. Akiyama, *Chem. Commun.* **2017**, *53*, 2966–2969.
- [12] a) S. Shinkai, A. Sugasaki, M. Ikeda, M. Takeuchi, *Acc. Chem. Res.* **2001**, *34*, 494–503; b) A. Ikeda, R. Funada, K. Sugikawa, *Org. Biomol. Chem.* **2016**, *14*, 5065–5072.
- [13] B. Perlmutter-Hayman, *Acc. Chem. Res.* **1986**, *19*, 90–96.
- [14] a) J. Gu, L. Cai, S. Tanaka, Y. Otsuka, H. Tabata, T. Kawai, *J. Appl. Phys.* **2002**, *92*, 2816–2820; b) Y. Okahata, T. Kobayashi, K. Tanaka, M. Shimomura, *J. Am. Chem. Soc.* **1998**, *120*, 6165–6166; c) A.-H. Bae, T. Hatano, K. Sugiyasu, T. Kishida, M. Takeuchi, S. Shinkai, *Tetrahedron Lett.* **2005**, *46*, 3169–3173; d) S. Ogasawara, A. Ikeda, J. Kikuchi, *Chem. Mater.* **2006**, *18*, 5982–5987.
- [15] a) H. Baker, P. Hambright, L. Wagner, *J. Am. Chem. Soc.* **1973**, *95*, 5942–5946; b) J. Mosinger, L. Slavětinská, K. Lang, P. Coufal, P. Kubáte, *Org. Biomol. Chem.* **2009**, *7*, 3797–3804.
- [16] A. K. Covington, M. Paabo, R. A. Robinson, R. G. Bates, *Anal. Chem.* **1968**, *40*, 700–706.
- [17] J. L. Butour, J. P. Macquet, *Eur. J. Biochem.* **1977**, *78*, 455–463.

## Entry for the Table of Contents



5,10,15,20-Tetra(4-pyridyl)porphyrin (**1**) in the **1**•TMe- $\beta$ -CDx complex was released from two TMe- $\beta$ -CDx cavities and intercalated into DNA under acidic conditions. A cationic **1** born by protonation of the 4-pyridyl moiety causes destabilisation of the **1**•TMe- $\beta$ -CDx complex and stabilisation of the intercalation of **1** into anionic DNA. In contrast, the DNA-intercalated **1** returned to the TMe- $\beta$ -CDx cavities by the deprotonation of **1** under neutral pH conditions. The reaction was repeatedly reversible by changing the pH.